



Regular Article

CFD Modeling and Industrial Evaluation of a Cyclone Cascade for the Production of the HDPE Catalyst

S. Ovaysi^{1,2*}

¹ Faculty of Petroleum and Chemical Engineering, Razi University, Kermanshah, Iran

² Enhanced Oil Recovery Division, Advanced Chemical Engineering Research Center, Razi University, Kermanshah, Iran

ARTICLE INFO

Article history:

Received: 2021-10-31

Accepted: 2022-01-10

Available online: 2022-04-21

Keywords:

Cyclone Separator,
CFD Modeling,
Flow Symmetry,
Particle Laden Flow,
HDPE Catalyst

ABSTRACT

A new approach is proposed to evaluate various designs for gas-solid cyclone separators. This approach uses single-phase flow simulation results to find a quantitative measure of flow symmetry in a given cyclone. Flow symmetry is computed by averaging imbalances of non-axial velocities throughout the cyclone. Using this approach, two standard design methods are evaluated and the cyclone with a more symmetric flow pattern is chosen as a starting point for further design improvements by reducing the diameter of its vortex finder. Two-phase computational fluid dynamics (CFD) simulations compute 90.2 % collection efficiency for the improved design. CFD simulations reveal using a cascade of four cyclones results in an overall 99.98 % collection efficiency. Once installed in the actual industrial setting, the cyclone cascade achieves a 98.56 % collection efficiency and a particle size distribution which is in good agreement with CFD computed results.

DOI: 10.22034/ijche.2022.312897.1413 URL: http://www.ijche.com/article_143126.html

1. Introduction

High density polyethylene (HDPE) is mainly produced through catalytic polymerization of ethylene in a slurry phase reactor where ethylene monomers react on the active sites of heterogeneous catalyst particles [1]. Hence, continuous production of solid catalysts is essential to maintaining the plant output. In a recent research and development project, a new production line for the HDPE catalyst was

designed and put into operation at Kermanshah polymer company. The new catalyst is supported on a zinc compound which is provided in coarse grains that have to be crushed into fine powder with a desired particle size distribution (PSD). It should be noted that the PSD of the catalyst support directly influences that of the catalyst particles which in turn has profound impacts on plant operations as well as the properties of the

*Corresponding author: s.ovaysi@razi.ac.ir (S. Ovaysi)

produced HDPE. To reach the desired PSD, a jet mill is employed where high pressure streams of nitrogen act on the original coarse particles. The outlet stream from the jet mill consists of nitrogen gas loaded with fine solid particles at pressures slightly above atmospheric. Thus, the fine powder has to be collected from the gas stream for further processing. Owing to their compact size, ease of operation and low maintenance costs, cyclone separators are considered the best choice for separation of fine solid particles from the above-mentioned particle laden flow. Furthermore, in order to achieve maximum collection of the fine powder produced by the jet mill, a cascade of cyclone separators is preferred. This study presents the cyclone design and evaluation phase of the above-mentioned research and development project at Kermanshah Polymer Company.

Formation of an outer quasi-free vortex concentric with an inner quasi- forced vortex is a fundamental requirement for the success of cyclonic separation [2]. High separation efficiencies are achieved if the above-mentioned vortices extend throughout the entire length of cyclone separators. Deviation of these vortices from longitudinal axis costs heavily in the efficiency of cyclonic separation. Previous studies highlighted the effects of inlet dimensions on flow pattern symmetry and, consequently, on the separation efficiency of cyclone separators [3, 4]. Furthermore, any shortcut flow carrying solid particles across the vortices and directly to the cyclone overflow has negative impacts on the separation efficiency [5]. Additionally, cyclone separators with non-circular geometries are proven to achieve superior collection efficiencies compared to conventional cyclone separators [6, 7]. Also, the geometry of the vortex finder is found to

significantly influence the cyclonic collection efficiency [8]. In light of the issues discussed, the design and manufacture of a cyclone separator require in-depth knowledge of its internal flow patterns. The computational fluid dynamics modeling is a potential tool to shed light on flow patterns inside a cyclone separator. Proper application of CFD to real life engineering problems involves not only a genuine knowledge of the mass, momentum, and energy conservation laws but also a thorough understanding of the relevant mathematics.

In this study, first, the design and CFD modeling of cyclones for the above-mentioned research and development project are discussed. Then, a new approach is presented to quantify symmetry and hence assess the collection efficiency of the designed cyclones using only single-phase CFD simulations. An improved design is then proposed and the CFD predictions are compared with the results obtained industrially after manufacturing and installing a cyclone cascade. This is then followed by conclusions.

2. Cyclone design

Table 1 summarizes the operating conditions of the particle laden flow delivered by the jet mill employed in the plant. It has to be stressed that the carrier gas is composed of industrial grade nitrogen. Additionally, particle size distribution (PSD) of the fine powder in this stream, suggested by the jet mill manufacturer, is shown in Figure 1. Solid particles in the stream characterized above need to be collected in a cyclone cascade composed of four cyclone separators in series. Individual cyclones were initially designed based on the guidelines suggested by [9, 10] and [11]. Given that the inlet gas flow rate for all cyclones is identical, the exact same design is

used for all four cyclones in Figure 2. Figure 3 presents a schematic diagram of a cyclone separator where the relevant dimensions are shown. Based on an inlet velocity of 15 m/s and the operating conditions in Table 1, a Stairmand cyclone with $D = 216$ mm and a Shepherd&Lapple cyclone with $D = 193$ mm were designed.

Table 1

Operating conditions of the particle-laden flow.

Property	Value
Pressure (barg)	0.3
Gas flow rate (NM ³ /hr)	300
Particles flow rate (Kg/hr)	10.4
Density of solid particles (Kg/m ³)	1010

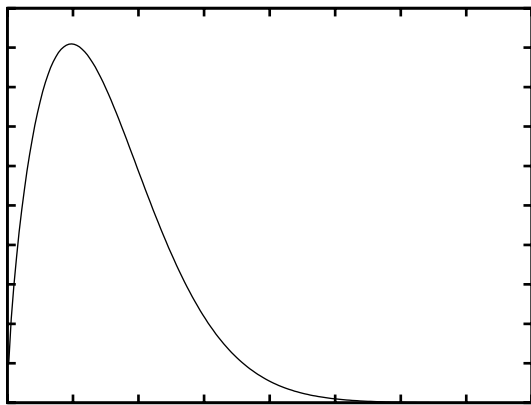


Figure 1. Particle size distribution of the feed stream to the first cyclone.

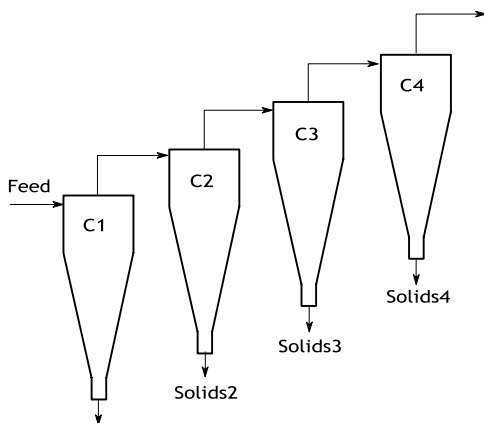


Figure 2. Schematic diagram of a cascade of four cyclone separators.

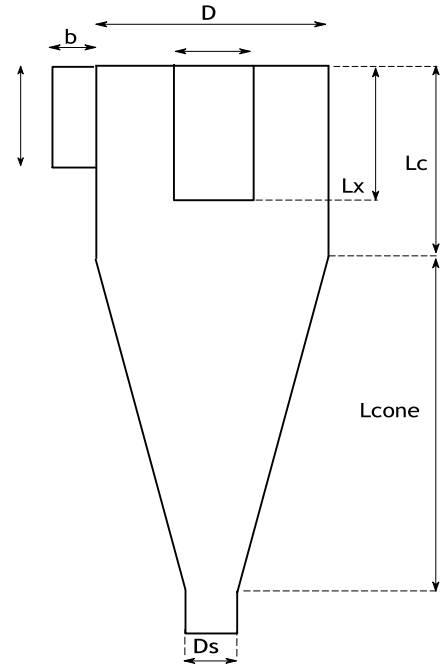


Figure 3. Schematic diagram of a cyclone separator.

3. CFD modeling

Due to the small pressure drops expected, incompressible fluid flow conditions were assumed for the carrier gas. The flow of an incompressible fluid is governed by Reynolds averaged continuity and momentum balance equations given by [12]:

$$\frac{\partial \bar{u}_i}{\partial x_i} = 0 \tag{1}$$

$$\frac{\partial \bar{u}_i}{\partial t} + u_j \frac{\partial \bar{u}_i}{\partial x_j} = -\frac{1}{\rho} \frac{\partial P}{\partial x_i} + \nu \frac{\partial u_j}{\partial x_j \partial x_i} - \frac{\partial R_{ij}}{\partial x_j} \tag{2}$$

where u and \bar{P} denote average values of velocity and pressure, respectively.

ρ and ν are density and kinematic viscosity respectively. Additionally, $R_{ij} = \overline{u'_i u'_j}$ denotes the Reynolds stress tensor and $u'_i = u_i - \bar{u}_i$ denotes the fluctuating velocity component.

Turbulent nature of the flow patterns inside cyclone separators necessitates using a model to take account of linear as well as angular momentums. The Reynolds stress turbulence model (RSM) [13] is proven to be accurate for

this purpose [14-16] as it requires the solution of the conservation equations for all Reynolds stress components. This model computes R_{ij} using Equation 3.

$$\frac{\partial R_{ij}}{\partial t} + \bar{u}_k \frac{\partial R_{ij}}{\partial x_k} = \frac{\partial}{\partial x_k} \left(\frac{v_t}{\sigma^k} \frac{\partial R_{ij}}{\partial x_k} \right) - \left[R_{ik} \frac{\partial \bar{u}_j}{\partial x_k} + R_{jk} \frac{\partial \bar{u}_i}{\partial x_k} \right] - C_1 \frac{\epsilon}{K} \left[R_{ij} - \frac{2}{3} \delta_{ij} K \right] - C_2 \left[P_{ij} - \frac{2}{3} \delta_{ij} P \right] - \frac{2}{3} \delta_{ij} \epsilon \quad (3)$$

$$P_{ij} = - \left[R_{ik} \frac{\partial \bar{u}_j}{\partial x_k} + R_{jk} \frac{\partial \bar{u}_i}{\partial x_k} \right], \quad P = \frac{1}{2} P_{ij} \quad (4)$$

where P and v_t denote the fluctuating kinetic energy production and kinematic eddy viscosity, respectively. The empirical parameters $\sigma^k = 1$, $C_1 = 1.8$, and $C_2 = 0.6$ are taken constant. Also, ϵ is the turbulence dissipation rate obtained using:

$$\frac{\partial \epsilon}{\partial t} + \bar{u}_j \frac{\partial \epsilon}{\partial x_j} = \frac{\partial}{\partial x_j} \left[\left(v + \frac{v_t}{\sigma^\epsilon} \right) \frac{\partial \epsilon}{\partial x_j} \right] - C^{\epsilon_1} \frac{\epsilon}{K} R_{ij} \frac{\partial \bar{u}_i}{\partial x_j} - C^{\epsilon_2} \frac{\epsilon^2}{K} \quad (5)$$

where $K = \frac{1}{2} \overline{u_i' u_i'}$ denoted the fluctuating kinetic energy. The empirical constants are $\sigma^\epsilon = 1.3$, $C^{\epsilon_1} = 1.44$, and $C^{\epsilon_2} = 1.92$.

Furthermore, due to the low particle loading in the cyclones studied, i.e., the volume fraction of solids $< 10 - 12 \%$, a discrete phase modeling (One way coupling) technique is used to track the solid particles. Using this approach, the particle motion is governed by:

$$\frac{\partial u_{pi}}{\partial t} = \frac{18\mu}{\rho_p d_p^2} \frac{C_D Re_p}{24} (u_i - u_{pi}) + \frac{g_i(\rho_p - \rho)}{\rho_p} \quad (6)$$

$$\frac{dx_{pi}}{dt} = u_{pi} \quad (7)$$

where index p is used to denote particle properties. Additionally, d_p , C_D , and Re_p are the particle diameter, drag coefficient, and particle Reynolds number respectively. Particle Reynolds number is calculated based on the relative particle velocity and is given by:

$$Re_p = \frac{\rho_p d_p |u - u_p|}{\mu} \quad (8)$$

A time integration scheme along the trajectory of individual particles yields the position of particles at any given time. This technique is used to calculate the collection efficiencies reported in this study.

To assess the collection efficiencies of the above-mentioned designs, a series of CFD simulations was carried out under varying operating conditions. Ansys Fluent 16.1 was used to perform the simulations. Table 2 summarizes the boundary conditions used for both gas and solid phases. The RSM turbulence model together with the quadratic pressure strain was used in the present study. Pressure-velocity coupling was performed using the SIMPLE scheme. Furthermore, the spatial discretizations applied in CFD simulations are listed in Table 3. It has to be mentioned that 418,706 and 567,741 tetrahedral cells were sufficient to achieve grid independent results for Stairmand and Shepherd&Lapple designs respectively.

Table 2
Boundary conditions used for gas and solid phases.

Boundary type	Gas phase	Solid Phase
Inlet	Constant velocity	Escape
Overflow	Outflow	Escape
Underflow	Wall	Trap
Walls	Wall	Reflect

Table 3

Spatial discretizations applied in CFD simulations.

Variable	Spatial discretization
Gradient	Least squares cell based
Pressure	PRESTO
Momentum	First order upwind
Turbulent kinetic energy	First order upwind
Turbulent dissipation rate	First order upwind
Reynolds stress	First order upwind

4. Results and discussion

4.1. Design improvements

To arrive at the best starting point in designing the above-mentioned cyclone separators, the two standard designs introduced in section 2 were analyzed using single-phase CFD simulations with identical boundary conditions (see Table 2). Figures 4 and 5 show the contour plots of velocities for these two standard designs. Evidently, both the inner and outer vortices deviate from the longitudinal axis in both cyclones. As noted earlier, this phenomenon is one of the factors that greatly lowers the collection efficiency of cyclonic separation. However, a quantitative measure is needed to judge the symmetry of vortices and hence collection efficiencies of various cyclone separators using single-phase flow simulations alone. Equation 9 is proposed to make such quantitative comparisons.

$$E = |\mathbf{u} \cdot \mathbf{d}_{\perp \text{axis}}| \quad (9)$$

where d and u denote distance from axis and non-axial velocity on the plane perpendicular to axial direction of the cyclone respectively. E denotes the asymmetry of flow patterns inside the cyclone. Smaller values of E indicate more symmetric flow patterns. Additionally, a perfectly symmetric flow pattern yields $E = 0$. Since the x -axis is axial direction in all cyclones of this study, Equation 9 is simplified

to:

$$E = \left| \mathbf{u} \cdot \mathbf{d}_{y-z \text{ plane}} \right| = \left| \frac{1}{N} \sum_i ((y_i - y_0)|u_{y,i}| + (z_i - z_0)|u_{z,i}|) \right| \quad (10)$$

where i enumerates over all interior points occupied by fluids and N is the total number of points. y_0 and z_0 denote the coordinates of the axis of cyclone. It should be noted that, to avoid asymmetries due to using a single entrance conduit, this equation is applied only to the areas below the vortex finder in all cyclones studied here.

Figure 6 shows distributions of u_y and u_z in the Shepherd&Lapple and Stairmand designs. The visual comparison of figures 6(a) and 6(b) against Figures 6(c) and 6(d) reveals a better symmetry for the Stairmand design. This is numerically confirmed by using equation 10 which yields $E = 0.0019$ and $E = 0.0016 \text{ m}^2/\text{s}$ for the Shepherd&Lapple and Stairmand designs respectively. Additionally, two-phase flow simulations reveal 61.5 % and 68.6 % collection efficiencies for the Shepherd&Lapple and Stairmand designs respectively. Therefore, the Stairmand design achieves a more symmetric flow pattern and hence a better collection efficiency which is in agreement with the findings of previous studies [5, 12]. However, flow patterns inside this cyclone is still asymmetric to an extent that

vortices impinge on the walls and disperse any collected solid particles into the moving fluid

(See Figure 5). Therefore, a low collection efficiency is expected from this design.

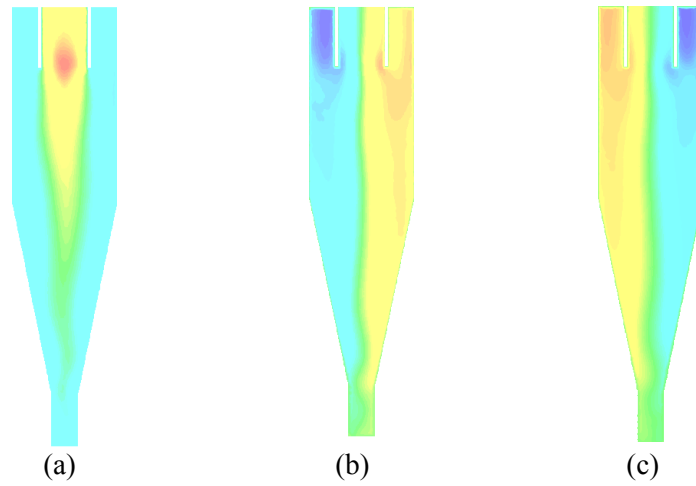


Figure 4. Contours of a) -10  20 m/s: u_x on z-x plane, b) -21  21 m/s: u_y on z-x plane, and c) -24.5  24.5 m/s: u_z on y-x plane in the Shepherd&Laple design.

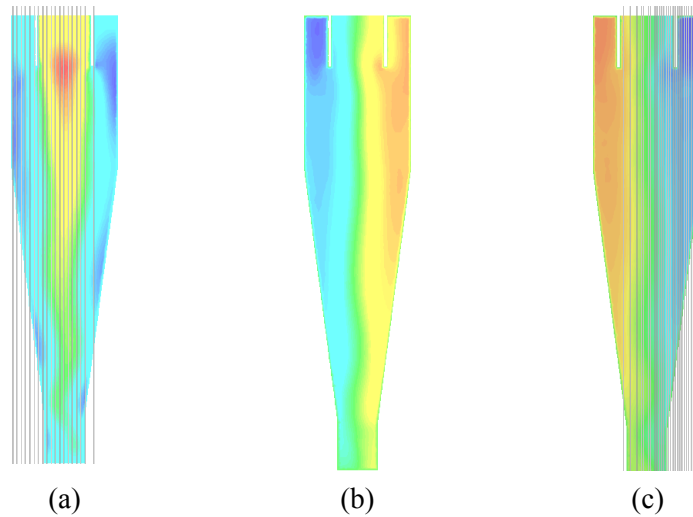
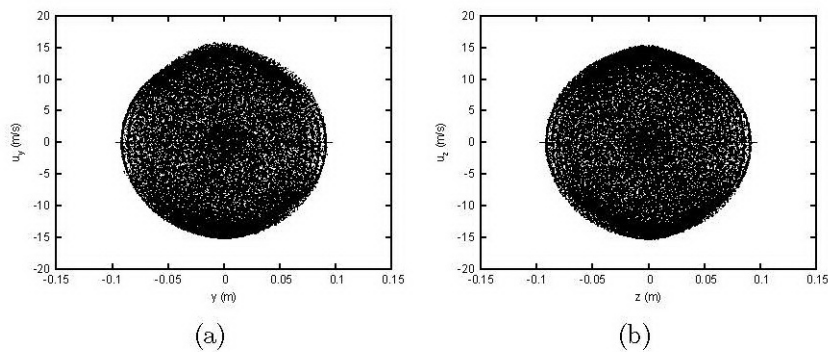


Figure 5. Contours of a) -5  13 m/s: u_x on z-x plane, b) -21  21 m/s: u_y on z-x plane, and c) -23  23 m/s: u_z on y-x plane in the Stairmand design.



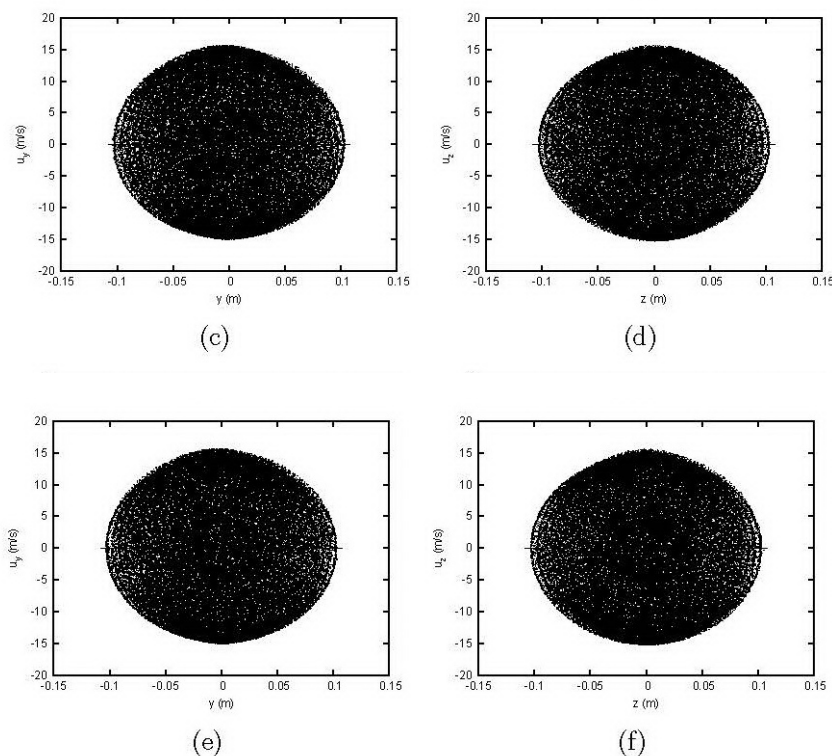


Figure 6. a), c), and e) distributions of u_y along y-axis in Shepherd&Lapple, Stairmand and improved designs respectively. b), d), and f) distributions of u_z along z-axis in the Shepherd&Lapple, Stairmand and improved designs respectively.

To improve the Stairmand design, reduction of the vortex finder diameter is proposed [17, 16]. Therefore, the vortex finder diameter is reduced from 100 mm to 92 mm in the modified design (the vortex finder is constructed from a 4 mm thick material). This led to major improvements in flow symmetry as illustrated in Figure 7 where the impingement of vortices on cyclone walls is quite negligible. Additionally, Figures 6(e) and 6(f) demonstrate more symmetric velocity distributions in the modified design which, using equation 10, yield $E = 0.00081 \text{ m}^2/\text{s}$. This proves that the flow pattern in the improved design is more symmetric and the entrained solid particles are exposed to a symmetric centrifugal force all along the cyclone. This is confirmed by the symmetry of pressure profiles at various distances from top of the cyclone as shown in Figure 8.

Furthermore, computed particle trajectories reveal a 90.2 % collection efficiency for a single cyclone. Also, Table 4 reports the CFD predictions of inlet and outlet flowrates of solid particles for all the four cyclones in cascade as well as their collection efficiencies. Given a predicted 99.98 % collection efficiency for a cascade of four cyclones, design improvements are finalized at this step. Table 5 reports the finalized geometry of the improved cyclone. It has to be mentioned that each cyclone adds a 600 Pa pressure drop to the gas stream.

Due to immediate industrial implementation of the above-mentioned design, it is necessary to examine how collection efficiencies change with $\pm 5 \%$ variations in velocity, density and viscosity resulting from changes in operating conditions, i.e., the flow rate, temperature, and pressure. CFD simulations reveal no

significant changes in collection efficiencies with $\pm 5\%$ variations of velocity. Impacts of density and viscosity variations on collection efficiencies are illustrated in Figure 9. It is observed that $\pm 5\%$ variations in the density and viscosity of the carrier gas has negligible impact on the collection efficiency of the cyclone designed in this study. Additionally, in order to understand what extent of density and viscosity variations has significant impacts on the collection efficiency, density and viscosity were varied from 1.487 to 29.74 Kg/m^3 and 1.66×10^{-5} to 1.33×10^{-4} Pa.s respectively. Figure 9(a) shows that such a large variation in density has insignificant impact on the

collection efficiency. However, large variations in viscosity greatly impacts the collection efficiency as shown in Figure 9(b). Reduction of the collection efficiency in a more viscous medium is explained by an increase in viscous drag acting on solid particles. This prevents the separation of solid particles from the bulk of gas caused by centrifugal forces resulting from the two concentric vortices. Moreover, a more viscous carrier gas is less likely to experience a strong vortex under the same operating conditions compared to a less viscous carrier gas. Therefore, centrifugal forces in the cyclone become weaker as viscosity increases.

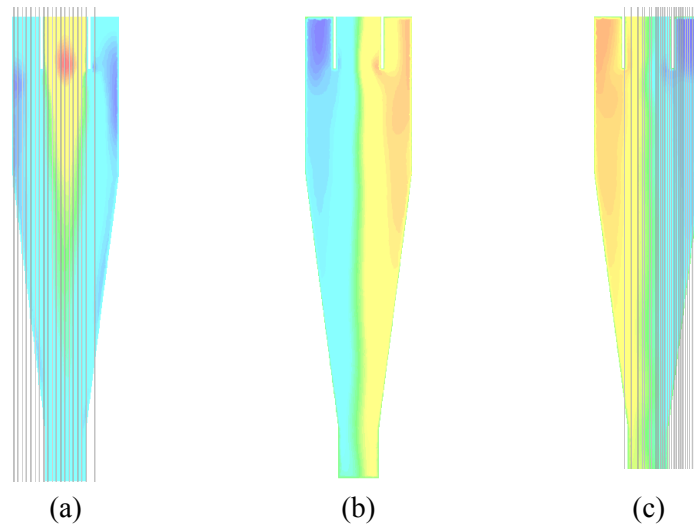


Figure 7. Contours of a) -5  17.5 m/s: u_x on z-x plane, b) -20  20 m/s: u_y on z-x plane, and c) -22.5  22.5 m/s: u_z on y-x plane in the improved design.

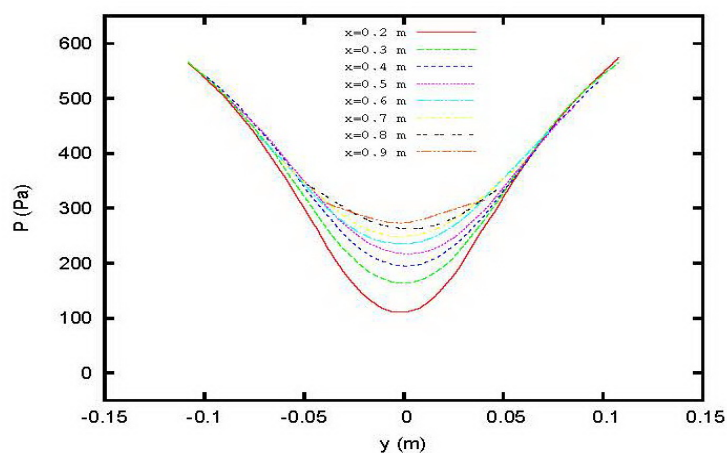


Figure 8. Pressure profiles at various y-z planes along axial direction in the improved design.

Table 4

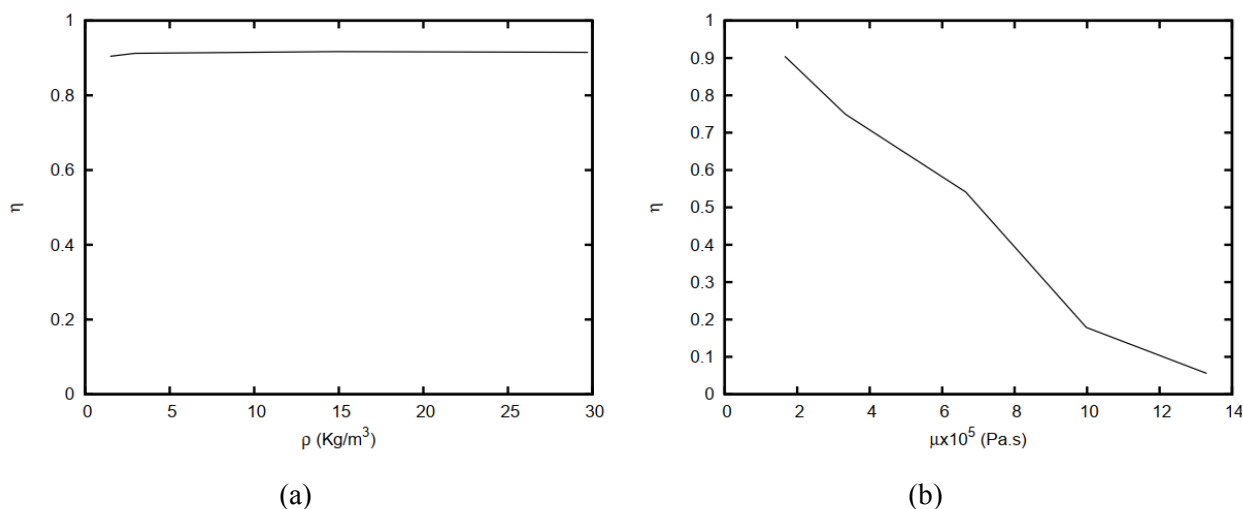
CFD predicted collection efficiencies for four cyclones in a cascade.

Cyclone	Solids at inlet (Kg/s)	Collected Solids (Kg/s)	Collection efficiency (%)
1	0.003	0.002706	90.2
2	0.000294	0.0002183	72.77
3	0.00008158	0.00005896	72.27
4	0.0000226	0.00001623	71.81
1-4	0.003	0.00299949	99.98

Table 5

Geometric dimensions of the improved cyclone separator.

Dimension	Value (mm)
D	216
L_c	324
L_{cone}	540
L_x	108
D_e	92
D_s	81
a	108
b	43

**Figure 9.** Impacts of a) density and b) viscosity variations on the collection efficiency.

4.2. Industrial evaluation

Four cyclone separators with the exact dimensions of the above-mentioned improved design were fabricated using stainless steel material. These cyclones were then installed in series with the first cyclone receiving its feed stream from a jet mill. Rotameters were used to measure the nitrogen flow to the jet mill and

consequently to the first cyclone. The solids flow to the jet mill was carefully controlled using a double-screw feeder at the top. Mass balance calculations reveal that out of 700 Kg solids fed to the jet mill, a sum of 690 Kg is collected from the cascade of four cyclones. This yields 98.6 % for the collection efficiency of the cascade which is in good agreement with

99.98 % computed from CFD simulations. Furthermore, samples were taken from the collected solids from the first cyclone and sent for the PSD analysis. This analysis was performed using a HORIBA laser scattering particle size distribution analyzer LA-960. Figure 10 compares this PSD with that computed from CFD simulations. Additionally, the PSDs of solids in the feed

stream and overflow (computed from CFD simulations) of the first cyclone are plotted in this figure. It is clear that the installed cyclone cascade achieves excellent collection efficiency. Moreover, CFD simulations successfully predict this efficiency and hence are extremely useful in the real-world applications of this type.

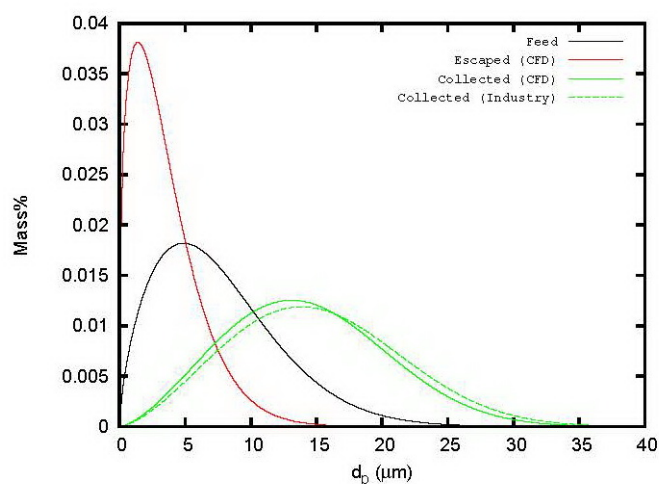


Figure 10. Particle size distributions of the streams entering and exiting the first cyclone.

5. Conclusions

Computational fluid dynamics was employed to evaluate two standard cyclone separator designs, namely the Shepherd&Lapple and Stairmand designs. A new approach was proposed to quantify flow symmetry in a given cyclone using single-phase CFD simulations alone. This greatly reduces the computational cost compared to two-phase simulations. Using the new approach, the absolute values of non-axial fluid velocities are integrated over the entire medium. Asymmetric flow patterns are then identified by nonzero values for the resulting integral. Using this approach, the Stairmand design was found superior to the Shepherd&Lapple design. This design was then improved by reducing its vortex finder diameter to yield a more symmetric flow pattern inside the cyclone. The collection

efficiency of the cyclone was computed using two-phase CFD simulations which yield 90.2 % for a single cyclone. Further improvements in the CFD computed collection efficiency up to 99.98 % was obtained by using a cascade of four identical cyclones. The cyclone cascade was manufactured and installed at the downstream of a jet mill in Kermanshah Polymer Company. Operational tests reveal 98.6 % collection efficiency for the actual cyclone cascade which runs continuously and trouble-free after several months of operation. This level of agreement between CFD predictions and the results from industry proves that CFD, once combined with thorough understanding of flow patterns in a cyclone, is a valuable tool in designing efficient cyclone separators.

Acknowledgement

Financial support for this study was provided by Kermanshah Polymer Company. Their support is greatly appreciated.

References

- [1] Khare, N. P., Seavey, K. C. and Liu, Y. A., "Steady state and dynamic modeling of commercial slurry high density polyethylene (HDPE) processes", *Industrial and Engineering Chemistry Research*, **41**, 5601 (2002).
- [2] Cui, J., Chen, X., Gong, X. and Yu, G., "Numerical study of gas-solid flow in a radial-inlet structure cyclone separator", *Industrial and Engineering Chemistry Research*, **49**, 5450 (2010).
- [3] Zhao, B., Su, Y. and Zhang, J., "Simulation of gas flow pattern and separation efficiency in cyclone with conventional single and spiral double inlet configuration", *Chemical Engineering Research and Design*, **84** (A12), 1158 (2006).
- [4] Elsayed, K. and Lacor, C., "The effect of cyclone inlet dimensions on the flow pattern and performance", *Applied Mathematical Modelling*, **35**, 1952 (2011).
- [5] Lee, J. W., Yang, H. J. and Lee, D. Y., "Effect of cylinder shape of a long coned cyclone on the stable flow-field establishment", *Powder Technology*, **165**, 30 (2006).
- [6] Su, Y., Zhao, B. and Zheng, A., "Simulation of turbulent flow in square cyclone separator with different gas exhaust", *Industrial and Engineering Chemistry Research*, **50**, 12162 (2011).
- [7] Zhang, T., Liu, C., Guo, K., Liu, H. and Wang, Z., "Analysis of flow field in optimal cyclone separators with hexagonal structure using mathematical models and computational fluid dynamics simulation", *Industrial and Engineering Chemistry Research*, **55**, 351 (2015).
- [8] Lim, K. S., Kim, H. S. and Lee, K. W., "Characteristics of the collection efficiency for a cyclone with different vortex finder shapes", *Journal of Aerosol Science*, **35**, 743 (2004).
- [9] Shepherd, C. B. and Lapple, C. E., "Flow pattern and pressure drop in cyclone dust collectors", *Journal of Industrial and Engineering Chemistry*, **31** (8), 972 (1939).
- [10] Shepherd, C. B. and Lapple, C. E., "Flow pattern and pressure drop in cyclone dust collectors", *Journal of Industrial and Engineering Chemistry*, **32**, 1246 (1940).
- [11] Stairmand, C. J., "The design and performance of cyclone separators", *Transactions of the Institution of Chemical Engineers*, **29**, 356 (1951).
- [12] Safikhani, H., Akhavan-Behabadi, M. A., Shams, M. and Rahimyan, M. H., "Numerical simulation of flow field in three types of standard cyclone separators", *Advanced Powder Technology*, **21**, 435 (2010).
- [13] Andersson, B., Andersson, R., Hakansson, L., Mortensen, M., Sudiyo, R. and van Wachem, B., *Computational fluid dynamics for engineers*, Cambridge University Press, (2012).
- [14] Slack, M. D., Prasad, R. O., Bakker, A. and Boysan, F., "Advances in cyclone modelling using unstructured grids", *Chemical Engineering Research and Design*, **78** (8), 1098 (2000).
- [15] Chuaha, T. G., Gimbin, J. and Choong, T. S. Y., "A CFD study of the effect of cone dimensions on sampling aero cyclones performance and hydrodynamics",

- Powder Technology*, **162** (2), 126 (2006).
- [16] Elsayed, K. and Lacor, C., "Optimization of the cyclone separator geometry for minimum pressure drop using mathematical models and cfd simulations", *Chemical Engineering Science*, **65**, 6048 (2010).
- [17] Raoufi, A., Shams, M., Farzaneh, M. and Ebrahimi, R., "Numerical simulation and optimization of fluid flow in cyclone vortex finder", *Chemical Engineering and Processing*, **47**, 128 (2008).